光学学报

基于深度学习的光纤超短脉冲啁啾放大研究

隋皓[1]，朱宏娜[1*]，张妍[2]，罗斌[3]，邹喜华[3]

[1]西南交通大学物理科学与技术学院，成都 四川 610031；
[2]信号盲处理国家级重点实验室，成都 四川 610041；
[3]西南交通大学信息科学与技术学院，成都 四川 610031

摘要 全光纤超短脉冲啁啾放大技术在激光技术和超快光学领域备受关注。针对传统数值方法分析光纤中超短脉冲啁啾放大过程存在计算量大、效率低等问题，采用深度学习方法开展全光纤超短脉冲啁啾放大过程建模研究。首先分析脉冲啁啾量等参数对超短光脉冲传输过程的影响。预训练设计的深度神经网络模型，分析网络对不同初始脉冲啁啾量的预测精度，进一步探索了不同初始脉冲半峰全宽、峰值功率和啁啾量等复杂情况下网络的泛化性及预测精度。本研究拓宽了数据驱动方法在激光行为预测方面的应用，为光纤中超短脉冲的特性研究提供了新思路。

关键词 非线性光学；光纤参量啁啾脉冲放大；卷积神经网络；非线性薛定谔方程

中图分类号 O437　　**文献标志码** A　　**DOI:** 10.3788/AOS221454

1 引　言

超短超强的激光脉冲在超快光学及强光与物质相互作用等领域有重要应用[1-4]。其中，光参量啁啾脉冲放大（OPCPA）技术是一种广泛运用的超短、高功率脉冲放大技术[5-12]。OPCPA通常采用非线性晶体实现相位匹配的脉冲参量放大过程，该类系统复杂性高，存在脉冲窄化效应和热效应等[4-5,13-14]。全光纤的光纤参量啁啾脉冲放大（FOPCPA）技术是另一种被广泛研究的啁啾脉冲放大技术，通过光纤的非线性实现啁啾脉冲参量放大的过程[2,14-20]，FOPCPA可提供优异的增益带宽，采用更紧凑、稳定的系统设计实现超短脉冲的放大[2,14-15]。基于四波混频过程的FOPCPA过程可通过非线性薛定谔方程描述[2,18,21]。FOPCPA系统对初始参数和光纤参数非常敏感，较小的参数变化可导致超短光脉冲非线性传输过程的显著变化。通常，对超短脉冲放大过程的特性研究或设计优化需要借助分步傅里叶法等数值方法开展大量参数化模拟，但该方法存在系统复杂性高、效率低、计算量大等问题[21-22]。

近年来，基于数据驱动的深度学习方法成为光脉冲非线性传输过程建模及应用的研究热点。多种神经网络被应用于光纤中光脉冲非线性传输的建模[22-24]、光纤信道建模[25]、非线性补偿[26-27]等领域，并展现出下列优势[22,25]：1）深度学习方法可对缺少精确数学理论或物理模型的复杂传输场景进行数据驱动的建模，弥补常规模型驱动方法的不足；2）经过轻量化的深度神经网络可在实现高精度预测的同时大幅提升计算效率，减少算力需求；3）深度学习方法可实现光传输系统的端对端建模，避免常规模型驱动方法中函数结构嵌套、重复迭代等过程，有效降低仿真系统的复杂度。同时深度学习方法也被用于预测光纤参量放大过程中的光脉冲的传输及增益研究[28-29]。开展基于深度学习方法的FOPCPA建模，有利于拓展数据驱动方法在超短脉冲放大过程的应用，为超短超强光脉冲的产生、设计优化及特性研究提供思路。

本文开展基于深度学习方法的FOPCPA建模和超短光脉冲传输特性研究。分析FOPCPA系统中泵浦光、信号光的传输过程，并研究初始啁啾量对信号光放大过程的影响。预训练深度卷积神经网络，并验证其在不同初始脉冲啁啾量下的预测精度。最后探索在更复杂输入条件［如不同初始脉冲半峰全宽（FWHM）、峰值功率及啁啾量］下所设计的深度卷积神经网络的泛化性及预测精度。

2 基本原理

2.1 光纤参量啁啾脉冲放大原理

基于四波混频效应的光纤参量放大（FOPA）将泵浦光能量转移到信号光上以实现对信号光的放大，并产生共轭的闲频光，单泵浦FOPA过程可依据简并耦合非线性薛定谔方程[20-21]描述：

$$\frac{\partial A_1}{\partial z} + \frac{i}{2}\beta_{21}\frac{\partial^2 A_1}{\partial T^2} + \frac{1}{2}\alpha A_1 = i\gamma\left\{\left[|A_1|^2 + 2\left(|A_2|^2 + |A_3|^2\right)\right]A_1 + 2A_2 A_3 A_1^* \exp\left(i\Delta\beta z\right)\right\}, \tag{1}$$

$$\frac{\partial A_2}{\partial z} + \frac{i}{2}\beta_{22}\frac{\partial^2 A_2}{\partial T^2} + \frac{1}{2}\alpha A_2 = i\gamma\left\{\left[|A_2|^2 + 2\left(|A_3|^2 + |A_1|^2\right)\right]A_2 + A_3^* A_1^2 \exp\left(-i\Delta\beta z\right)\right\}, \tag{2}$$

$$\frac{\partial A_3}{\partial z} + \frac{i}{2}\beta_{23}\frac{\partial^2 A_3}{\partial T^2} + \frac{1}{2}\alpha A_3 = i\gamma\left\{\left[|A_3|^2 + 2\left(|A_2|^2 + |A_1|^2\right)\right]A_3 + A_2^* A_1^2 \exp\left(-i\Delta\beta z\right)\right\}, \tag{3}$$

式中：A_1、A_2 和 A_3 分别为泵浦光、信号光和闲频光脉冲包络的慢变振幅；α 为光纤的衰减系数；β_{21}、β_{22} 和 β_{23} 分别为泵浦光、信号光和闲频光的二阶色散系数；$\Delta\beta = \beta_2 + \beta_3 - 2\beta_1$ 为线性的相位匹配系数；γ 为光纤的非线性系数；T 为随脉冲以群速度移动的参照系中的时间度量；z 为传输距离。模拟中采用的典型光纤参数如表 1 所示[20]。

表 1 模拟中使用的典型光纤参数
Table 1 Typical fiber parameters used in simulation

Nonlinear coefficient / (km·W)	Fiber loss coefficient / km	Dispersion slope / (ps·nm⁻²·km⁻¹)	Zero dispersion wavelength /nm	Pump wavelength /nm	Signal wavelength /nm
15	0.05	0.02	1550	1553	1531

初始啁啾泵浦光和信号光脉冲分布[21]满足：

$$A_p(T, 0) = \sqrt{P_p}\exp\left(-\frac{1 + iC_p}{2}\cdot\frac{T^2}{T_0^2}\right), \tag{4}$$

$$A_s(T, 0) = \sqrt{P_s}\exp\left(-\frac{1 + iC_s}{2}\cdot\frac{T^2}{T_0^2}\right), \tag{5}$$

式中：P_p 和 P_s 分别为泵浦光和信号光的峰值功率；T_0 为泵浦光和信号光的脉冲半峰全宽；C_p 和 C_s 分别为泵浦光和信号光脉冲的初始啁啾参量。当 C_p、C_s、T_0、P_p 和 P_s 分别设置为 0、0、10 ps、1 W 和 0.01 mW 时，啁啾信号光和泵浦光脉冲的传输过程如图 1 所示。随着传输距离的增加，泵浦光能量逐步向信号光转移，实现啁啾脉冲的放大。随着光脉冲传输距离的增加，能量转换效率越来越高，泵浦光能量快速降低，信号光能量快速提高。
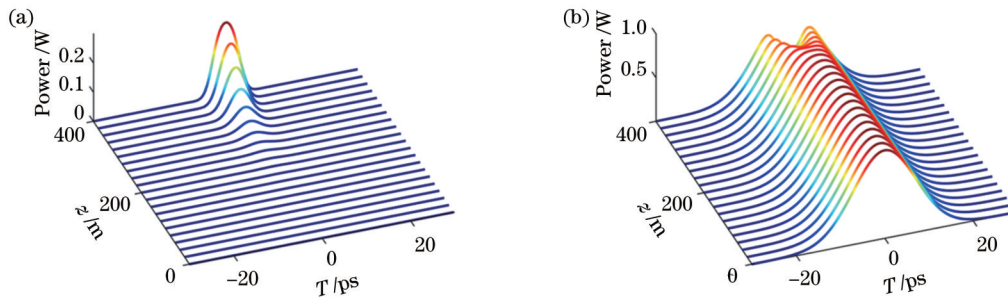

图 1 超短脉冲啁啾放大过程。(a)信号光传输；(b)泵浦光传输
Fig. 1 Ultrashort pulse chirp amplification process. (a) Signal pulse propagation; (b) pump pulse propagation

研究初始啁啾参量对信号光放大的影响，当 C_s 分别为 −10、0 和 10 时，信号光在传输距离为 100 m、200 m、300 m 和 400 m 处的归一化强度如图 2 所示。图 2(a)中，初始啁啾对前 100 m 的信号光传输影响较大。初始啁啾为负时，信号光被放大的同时脉宽展宽；初始啁啾为正时，信号光被放大的同时脉宽窄化，并产生两个次级峰值。图 2(c)、(d)中信号光传输 300 m 后，初始啁啾对信号光脉宽产生了较大影响，初始啁啾的正负决定了脉冲的压缩或展宽。此外，初始信号光峰值功率和 FWHM 也是影响传输过程的重要因素。

2.2 深度卷积神经网络结构

为实现光纤参量啁啾脉冲放大的建模，设计图 3 中的深度卷积神经网络。网络主体包含 5 个卷积块和 3 个全连接层。卷积块由一维卷积层、一维批归一化（BN）层、ReLU 激活函数和一维池化层组成。初始信号光脉冲分布 $A_s(T, 0)$ 作为神经网络的输入，经过 5 个卷积块和 3 个全连接层后，输出信号光脉冲分布为 $A_s(T, z_i)$，$i = 1, 2, \cdots, 400$。为更好地提取特征，将初始脉冲的实部和虚部共同作为深度卷积神经网络的输入。

训练过程中，网络通过一系列训练数据 $(y_i, x_i)(i = 1, 2, \cdots, n)$ 优化其映射函数 N_θ，则最优的深度卷积网络的映射函数为

$$N_{\theta^*} = \arg\min_{\theta\in\Theta}\left\|N_\theta(y_i) - x_i\right\|^2, \tag{6}$$

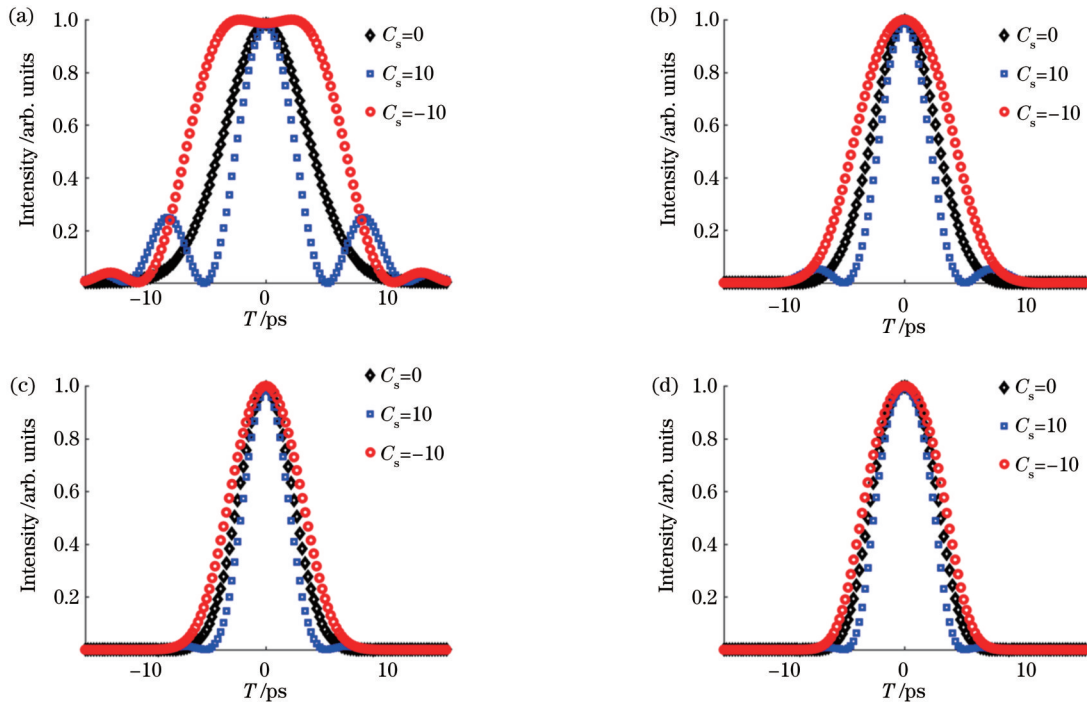式中：N_θ 为深度卷积网络的映射函数，由一系列网络权重组成；i 为训练集中样本数量；Θ 为 N_θ 的解空间。采用均方根误差计算网络预测结果与真实值的误差，

图 2　不同传输距离处的信号光归一化强度。(a) 100 m；(b) 200 m；(c) 300 m；(d) 400 m

Fig. 2　Normalized intensity of signal pulse at different propagation distance. (a) 100 m；(b) 200 m；(c) 300 m；(d) 400 m
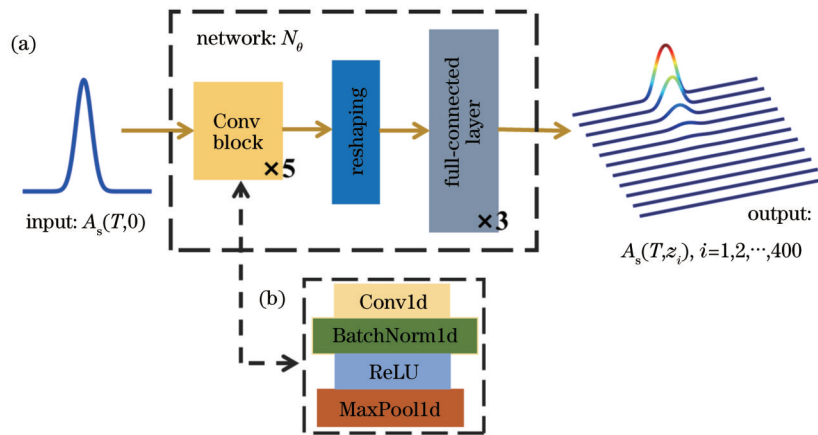

图 3　基于深度学习的超短脉冲啁啾放大预测。(a)深度卷积网络结构；(b)卷积块结构

Fig. 3　Predicting ultrashort pulse chirp amplification based on deep learning. (a) Deep convolutional network structure;
(b) convolutional block structure

并反向传播、更新网络权重。在网络训练中使用 Adam 优化器，并设置网络学习率为 1×10^{-4}。本文中网络搭建、训练及测试基于 Pytorch 平台完成。

3　结果分析与讨论

在多种数据集下开展网络的训练和测试，研究深度卷积神经网络在不同初始脉冲参数下的预测精度。采用分步傅里叶法（SSF）迭代求解式（1）～（3），获得数据集中所有样本。表 2 中给出了不同初始信号光参数的 4 种数据集。所有情况下的训练集和测试集相互独立，即不存在重复的样本。

考虑表 2 中情况 1，初始信号光的脉冲 FWHM 为 10 ps，峰值功率为 0.01 mW，C_s 的变化范围为 $-10\sim10$。在 10000 轮训练中，深度卷积神经网络在 40 个测试样本上的归一化误差如图 4 所示。所述误差为网络预测的光脉冲传输过程中误差与理论光脉冲传输过程中误差的差值，本质上误差来源于训练后的深度神经网络映射函数 N_θ 只能从理论上逼近所学习的物理过程，无法完全等效于非线性薛定谔方程系统。随着训练轮次的增加，网络权重逐步优化，深度卷积神经网络的预测误差逐渐减小。经过 2000 轮的训练，网络在测试数据集的归一化误差低于 1×10^{-6}。随着训练的继续进行，测试集上的损失平缓减小。在 10000 轮训练后，测试集的归一化误差低于 1×10^{-8}。

表 2　不同信号光脉冲参数的数据集
Table 2　Datasets with different signal pulse parameters

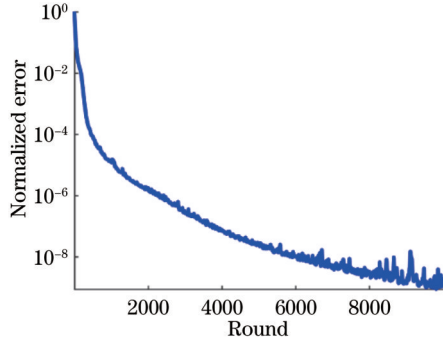| Case	Full width at half-maximum /ps	Peak power /mW	Chirp	Total sample number for training	Total sample number for testing
1	10	0.01	−10-10	161	40
2	8-12	0.01	−5-5	871	200
3	10	0.01-0.05	−5-5	871	200
4	8-12	0.01-0.05	−5-5	2041	500

图 4　不同 C_s 情况下测试集上的归一化误差
Fig. 4　Normalized error on testing set for different C_s

图 5 为 C_s＝−9 时预测的信号光传输过程、理论传输过程及网络预测值和理论值之差。对比图 5(a)、(b)，网络预测值和理论值相差极小。信号光在 400 m 的传输中，初始峰值功率从 0.01 mW 逐步放大至高于 0.20 W。如图 5(c)所示，整个脉冲放大的预测精度

高，最大误差低于 3.00 mW。结果表明，采用深度卷积神经网络可实现不同初始啁啾参量的信号光放大过程的精确预测。

进一步分析更复杂初始脉冲条件下 FOPCPA 的建模：分别是初始脉冲 FWHM 和啁啾参量改变的情况 2，初始脉冲峰值功率和啁啾参量改变的情况 3，初始脉冲 FWHM、峰值功率和啁啾参量均改变的情况 4。图 6 给出了 10000 轮训练中，3 种情况测试集上的归一化误差。随着网络训练轮次的增加，测试集上的误差均逐步减小。在情况 2 下，测试集上的损失减小得最快，经过 10000 轮训练，测试集上的归一化误差小于 $1×10^{-8}$。在初始脉冲功率变化(对应情况 3 和情况 4)时，网络收敛速度略有下降，这表明对不同初始信号光功率条件下 FOPCPA 建模难度高于不同初始信号光 FWHM 的情况。经过 10000 轮训练，第 3、4 种情况下测试集上的归一化误差低于 $1×10^{-7}$，均实现较高的预测精度。

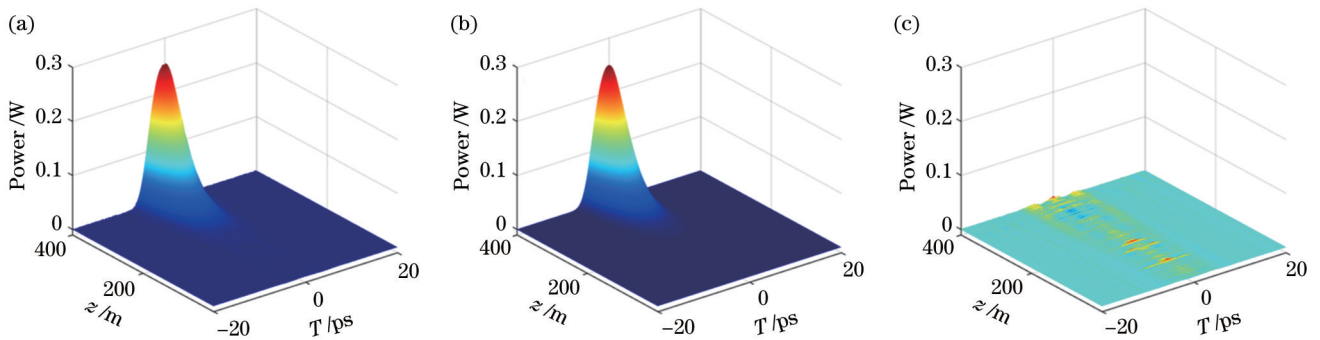图 5　C_s＝−9 时信号光脉冲传输过程。(a)网络预测结果；(b)理论结果；(c)预测结果和理论结果的差值
Fig. 5　Signal pulse propagation process when C_s＝−9. (a) Predicted result of network; (b) theoretical result; (c) difference between predicted result and theoretical result

不失一般性地选择情况 4 中对应初始 FWHM 为 8.8 ps、峰值功率为 0.02 mW、C_s＝−4 的样本，对网络预测的信号光脉冲传输过程、理论传输过程及网络预测值和理论值之差进行分析，对应的脉冲传输过程如图 7 所示。对比图 7(a)、(b)可知，网络预测的信号光放大过程与真实情况相当。如图 7(c)所示，网络预测误差主要集中在传输 350 m 后，且分布在脉冲峰值区域，最大的误差小于 10 mW。结果表明，在复杂的初始脉冲条件(不同初始 FWHM、峰值功率、啁啾参量)下，经过训练的深度卷积神经网络能精确预测信号光

放大传输过程，为超短脉冲放大传输过程及关键参数的定量研究提供有效的思路。

定量分析深度卷积神经网络在 4 种情况下的预测精度，采用归一化均方根误差(NRMSE)计算神经网络的预测值与理论值的差[22,26]：

$$R(x, \hat{x}) = \sqrt{\frac{\sum (x_{t,l} - \hat{x}_{t,l})^2}{\sum (x_{t,l})^2}}, \qquad (7)$$

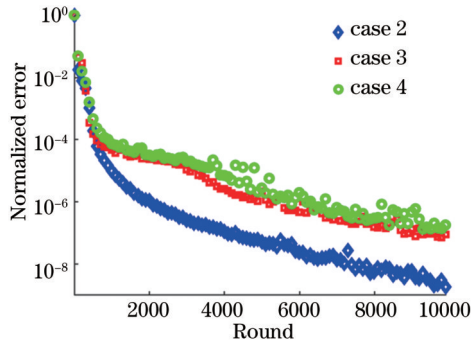式中：x 和 $\hat{x}$ 分别为信号光放大过程的理论值和网络预测值；$x_{t,l}$ 和 $\hat{x}_{t,l}$ 分别为在距离 l 和时间 t 时理论信号光

图 6 不同初始脉冲 FWHM 和 C_s，不同初始脉冲峰值功率和 C_s，不同初始脉冲 FWHM、峰值功率和 C_s 情况下测试集上的归一化误差

Fig. 6 Normalized error on testing sets in cases of different initial FWHM and C_s, different initial pulse power and C_s, and different initial FWHM, power, and C_s

幅值和网络预测的信号光功率。

表 3 列出了 2000、6000 和 10000 轮训练下 4 种情

况的 NRMSE 值。随着训练轮次的增加，4 种情况下测试数据集上的 NRMSE 误差逐步减小，与图 4、6 中网络损失曲线变化趋势一致。经过 10000 轮次的训练，在初始脉冲啁啾参量变化的情况 1 中，测试集上的 NRMSE 误差最小，仅为 0.0261。在最复杂的情况 4 中，初始脉冲 FWHM、峰值功率和啁啾参量同时变化，提出的神经网络模型经过 10000 轮次的训练，在 500 个测试样本上的 NRMSE 依然低于 0.0584。综上所述，本文方法精确实现了不同初始脉冲参数的全光纤啁啾脉冲放大传输建模。

表 3 不同情况下测试集上的 NRMSE
Table 3 NRMSE on testing set under different cases

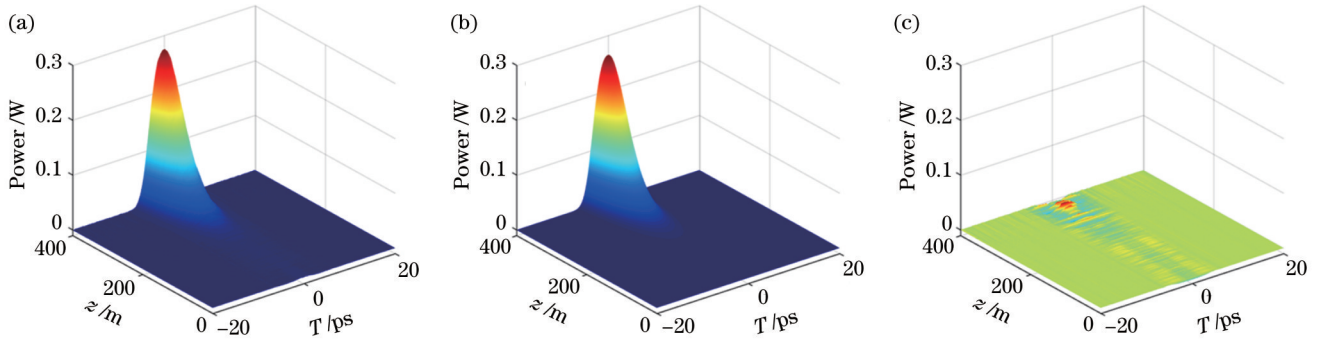| Epoch	NRMSE			
	Case 1	Case 2	Case 3	Case 4
2000	0.1349	0.1343	0.1797	0.2010
6000	0.0435	0.0585	0.0774	0.0920
10000	0.0261	0.0400	0.0497	0.0584

图 7 初始脉冲 FWHM 为 8.8 ps、峰值功率为 0.02 mW 和 $C_s=-4$ 时信号光脉冲传输。(a)预测结果；(b)理论结果；(c)预测结果和理论结果的差值

Fig. 7 Signal pulse propagation when FWHM, peak power, and C_s of initial pulse are 8.8 ps, 0.02 mW, and -4, respectively. (a) Predicted result; (b) theoretical result; (c) difference between predicted result and theoretical result

进一步比较深度卷积网络和常规分布傅里叶方法的计算效率，在相同计算资源下测试两种方法在表 2 中列出的 4 种情况下的计算时间。测试基于 Pytorch 平台完成，两种情况均采用 2080Ti GUP 加速计算。两种方法在 4 种情况下相同测试集上的归一化计算时间如表 4 所示。

在相同算力下：样本数量较小(情况 1)时，提出的深度学习网络的计算时间与常规方法相当；当样本数

表 4 不同情况下测试集上的归一化计算时间
Table 4 Normalized computing time on testing set for different cases

Method	Normalized computing time			
	Case 1	Case 2	Case 3	Case 4
SSF（split-step Fourier method）	1.01	4.79	4.93	11.76
Proposed deep learning method	1	1.14	1.15	1.45

量增加时，深度学习方法在计算效率上展现出巨大优势。在情况 4 中，提出的深度卷积网络对 500 个样本的脉冲放大传输建模的运算时间少于常规分步傅里叶方法运算时间的 1/10。结果显示，提出的轻量化网络在计算效率上相较常规数值方法优势明显。

4 结 论

基于深度学习方法开展全光纤超短啁啾脉冲放大建模研究。设计了由卷积块和全连接层组成的深度卷积神经网络，实现了不同的初始脉冲参数下全光纤啁啾脉冲放大传输的精确建模。首先分析了光纤参量啁啾脉冲放大过程及初始啁啾参量对脉冲传输的影响。研究了不同初始脉冲啁啾参量下，神经网络对信号光脉冲传输的预测精度。进一步研究了复杂初始脉冲设定情况下所提方法的有效性和稳定性。结果表明：经过 10000 轮训练，深度卷积神经网络在不同初始脉冲 FWHM、峰值功率和啁啾参量情况下达到 0.0584 的

归一化均方根误差，并实现了相较于常规数值方法 10 倍以上的计算效率提升。本文方法拓展了深度学习在激光技术和超快光学的应用，为超短超强光脉冲的传输特性研究提供思路。

参 考 文 献

[1] Genty G, Salmela L, Dudley J M, et al. Machine learning and applications in ultrafast photonics[J]. Nature Photonics, 2021, 15 (2): 91-101.

[2] Bigourd D, D'Augerès P B, Dubertrand J, et al. Ultra-broadband fiber optical parametric amplifier pumped by chirped pulses[J]. Optics Letters, 2014, 39(13): 3782-3785.

[3] 周朴, 冷进勇, 肖虎, 等. 高平均功率光纤激光的研究进展与发展趋势[J]. 中国激光, 2021, 48(20): 2000001.
Zhou P, Leng J Y, Xiao H, et al. High average power fiber lasers: research progress and future prospect[J]. Chinese Journal of Lasers, 2021, 48(20): 2000001.

[4] 叶荣, 阴明, 吴显云, 等. 光谱角色散 OPCPA 中啁啾脉冲频谱整形的理论研究[J]. 激光与光电子学进展, 2018, 55(4): 041901.
Ye R, Yin M, Wu X Y, et al. Theoretical study of spectrum shaping of chirped pulse in OPCPA with angular spectral dispersion[J]. Laser & Optoelectronics Progress, 2018, 55(4): 041901.

[5] 商景诚, 刘一州, 赵圣之, 等. 高重复频率光参量啁啾脉冲放大器研究进展[J]. 中国激光, 2021, 48(12): 1201004.
Shang J C, Liu Y Z, Zhao S Z, et al. High repetition-rate optical parametric chirped-pulse amplifiers[J]. Chinese Journal of Lasers, 2021, 48(12): 1201004.

[6] 李齐良, 朱殷芳, 金晶. 拉曼散射和偏振效应对光纤参量放大器增益的影响[J]. 中国激光, 2009, 36(s1): 61-65.
Li Q L, Zhu Y F, Jin J. The impact of stimulated Raman scattering and polarization effect on the gain of fiber optical parametric amplifier[J]. Chinese Journal of Lasers, 2009, 36(s1): 61-65.

[7] 曹华保, 王虎山, 袁浩, 等. 基于光参量放大的中红外飞秒光源进展(特邀)[J]. 光子学报, 2020, 49(11): 1149005.
Cao H B, Wang H S, Yuan H, et al. Research progress of mid-infrared femtosecond sources based on optical parametric amplification(invited)[J]. Acta Photonica Sinica, 2020, 49(11): 1149005.

[8] 李伟, 王道, 胡必龙, 等. 光学参量啁啾反转脉冲放大系统色散补偿方案[J]. 中国激光, 2020, 47(6): 0601008.
Li W, Wang X, Hu B L, et al. Dispersion-compensation scheme of optical parameter chirp reversal pulse amplification system[J]. Chinese Journal of Lasers, 2020, 47(6): 0601008.

[9] 王波鹏, 粟敬钦, 曾小明, 等. 参量荧光脉宽的理论与实验研究[J]. 光学学报, 2016, 36(5): 0519001.
Wang B P, Su J Q, Zeng X M, et al. Theoretical and experimental study on parametric fluorescence pulse width[J]. Acta Optica Sinica, 2016, 36(5): 0519001.

[10] 潘雪, 李学春, 王江峰, 等. 利用光参量啁啾脉冲放大进行任意光谱整形方案的稳定性分析[J]. 中国激光, 2011, 38(1): 0102004.
Pan X, Li X C, Wang J F, et al. Study on stability of arbitrary spectral shaping using optical parametric chirped pulse amplification[J]. Chinese Journal of Lasers, 2011, 38(1): 0102004.

[11] 李现华, 曾曙光, 张彬, 等. 啁啾匹配光参量啁啾脉冲放大理论分析[J]. 激光与光电子学进展, 2010, 47(7): 071901.
Li X H, Zeng S G, Zhang B, et al. Theoretical analysis on chirp matched optical parametric chirped pulse amplification[J]. Laser & Optoelectronics Progress, 2010, 47(7): 071901.

[12] 王艳海. 接近单周期量级的两级非共线光参量放大[J]. 光学学报, 2015, 35(8): 0819002.
Wang Y H. Two-stage noncollinear optical parametric amplification approaching single cycle[J]. Acta Optica Sinica, 2015, 35(8): 0819002.

[13] 李现华, 曾曙光, 张彬, 等. 啁啾匹配和同步抖动对光参量啁啾脉冲放大的影响[J]. 强激光与粒子束, 2010, 22(12): 2824-2828.
Li X H, Zeng S G, Zhang B, et al. Influence of chirp match and synchronization jitter on optical parametric chirped pulse amplification[J]. High Power Laser and Particle Beams, 2010, 22(12): 2824-2828.

[14] Bigourd D, Lago L, Kudlinski A, et al. Dynamics of fiber optical parametric chirped pulse amplifiers[J]. Journal of the Optical Society of America B, 2011, 28(11): 2848-2854.

[15] Bigourd D, Dutin C, Vanvincq O, et al. Numerical analysis of broadband fiber optical parametric amplifiers pumped by two chirped pulses[J]. Journal of the Optical Society of America B, 2016, 33(9): 1800-1807.

[16] Mussot A, Kudlinski A, D'Augères P B, et al. Amplification of ultra-short optical pulses in a two-pump fiber optical parametric chirped pulse amplifier[J]. Optics Express, 2013, 21 (10): 12197-12203.

[17] Vanvincq O, Fourcade-Dutin C, Mussot A, et al. Ultrabroadband fiber optical parametric amplifiers pumped by chirped pulses. Part 1: analytical model[J]. Journal of the Optical Society of America B, 2015, 32(7): 1479-1487.

[18] Fourcade-Dutin C, Vanvincq O, Mussot A, et al. Ultrabroadband fiber optical parametric amplifier pumped by chirped pulses. Part 2: sub-30-fs pulse amplification at high gain [J]. Journal of the Optical Society of America B, 2015, 32(7): 1488-1493.

[19] Zhu H N, Zhu Z Y, Li P P, et al. The analysis and optimization of broadband fiber optical parametric amplifiers pumped by chirped pulses[J]. IEEE Journal of Selected Topics in Quantum Electronics, 2019, 25(4): 3100108.

[20] Marhic M E. Fiber optical parametric amplifiers, oscillators related devices[M]. New York: Cambridge University Press, 2007: 146-181.

[21] Agrawal G P. Nonlinear fiber optics[M]. 4th ed. Amsterdam: Academic Press, 2007.

[22] Salmela L, Tsipinakis N, Foi A, et al. Predicting ultrafast nonlinear dynamics in fibre optics with a recurrent neural network [J]. Nature Machine Intelligence, 2021, 3(4): 344-354.

[23] Wang R Q, Ling L M, Zeng D L, et al. A deep learning improved numerical method for the simulation of rogue waves of nonlinear Schrödinger equation[J]. Communications in Nonlinear Science and Numerical Simulation, 2021, 101: 105896.

[24] Gautam N, Choudhary A, Lall B. Comparative study of neural network architectures for modelling nonlinear optical pulse propagation[J]. Optical Fiber Technology, 2021, 64: 102540.

[25] Wang D S, Song Y C, Li J, et al. Data-driven optical fiber channel modeling: a deep learning approach[J]. Journal of Lightwave Technology, 2020, 38(17): 4730-4743.

[26] Sui H, Zhu H N, Cheng L, et al. Deep learning based pulse prediction of nonlinear dynamics in fiber optics[J]. Optics Express, 2021, 29(26): 44080-44092.

[27] Sidelnikov O, Redyuk A, Sygletos S, et al. Advanced convolutional neural networks for nonlinearity mitigation in long-haul WDM transmission systems[J]. Journal of Lightwave Technology, 2021, 39(8): 2397-2406.

[28] Tay K G, Pakarzadeh H, Huong A, et al. Gain prediction of dual-pump fiber optic parametric amplifier based on artificial neural network[J]. Optik, 2022, 253: 168579.

[29] Sui H, Zhu H N, Wu J, et al. Modeling pulse propagation in fiber optical parametric amplifier by a long short-term memory network[J]. Optik, 2022, 260: 169125.

Ultrashort Chirped Pulse Amplification in Fiber Based on Deep Learning

Sui Hao[1], Zhu Hongna[1*], Zhang yan[2], Luo Bin[3], Zou Xihua[3]

[1]*School of Physical Science and Technology, Southwest Jiaotong University, Chengdu* 610031, *Sichuan, China*;

[2]*National Key Laboratory of Science and Technology on Blind Signal Processing, Chengdu* 610041, *Sichuan, China*;

[3]*School of Information Science & Technology, Southwest Jiaotong University, Chengdu* 610031, *Sichuan, China*

Abstract

Objective   Fiber optical parametric chirped pulse amplification (FOPCPA) is a widely studied ultrashort pulse amplification technique. The FOPCPA can provide excellent gain bandwidth and achieve ultrashort pulse amplification with a more compact and stable system design. The basic principle of the operation relies on a degenerate phase-matched four-wave mixing process involving one strong narrow-bandwidth pump wave, a weak stretched signal, and a generated idler wave. The FOPCPA process can be described by the nonlinear Schrodinger equation. However, the FOPCPA system is highly sensitive to the initial parameters and fiber parameters. Consequently, the traditional numerical methods (i. e. , split-step Fourier method and finite-difference method) of analyzing the ultrashort CPA in an FOPCPA system require a huge amount of computation and become less efficient. Nowadays, deep learning (DL) methods have been developed to model and predict nonlinear pulse dynamics and thereby reap the benefits of purely data-driven methods without any underlying governing equations. This study focuses on modeling the ultrashort CPA in fiber by a DL method. The proposed method is expected to broaden the application of DL methods in the prediction of laser behavior and provide an alternative for studying the characteristics of ultrashort pulses in fiber.

Methods   A deep convolutional neural network is constructed in the present study. This network contains three parts: five convolutional blocks, a reshaping layer, and three fully connected layers (Fig. 3). Each convolutional block contains a one-dimensional (1d) convolutional layer, a batch normalization layer, a rectified linear unit activation function, and a 1d max pooling layer. The intensity distribution of the initial chirped pulse is used as the input of the neural network. After five convolutional blocks and three fully connected layers, the predicted ultrashort pulse propagation is obtained. For better feature extraction, the real and imaginary parts of the initial pulse are simultaneously used as the input of the deep convolutional neural network. The weights and biases of the proposed network are updated by the back-propagation of the root-mean-square error between the predicted pulse propagation intensity and the ground truth. In the training phase, this study uses the Adam optimizer and sets the learning rate of the network to 0. 0001. The whole program is implemented in the Pytorch framework with a 2080Ti GPU. Four cases are considered to test the performance of the proposed network (Table 2). In all these cases, the training sets and testing sets are independent of each other, namely that no duplicate samples are used.

Results and Discussions   Specifically, the prediction precision in the four cases is discussed. As training epochs increase, network weights are gradually optimized, and the prediction error of the deep convolutional neural network is gradually reduced. After training for 10000 rounds, the normalized errors on the testing sets in the four cases are all smaller than 1×10^{-7} (Fig. 4 and Fig. 6). Even in the most complex case (different initial pulse power, width, and chirp), excellent visual agreement is achieved between the predicted pulse propagations and the real ones where all the temporal distributions include details. The prediction error is mainly concentrated in the propagation range after 350 m and is distributed in the range of the pulse peak, with a maximum value smaller than 10 mW (Fig. 7). In conclusion, the normalized root-mean-square errors of the 500 testing samples are smaller than 0. 0584. The results show that the proposed network can predict the process of ultrashort CPA under complex initial pulse conditions with high precision. Furthermore, the computation efficiency of the proposed DL method is investigated and compared with that of the traditional split-step Fourier method. The computation time of the proposed DL method for 500 independent samples is less than 1/10 that of the traditional split-step Fourier method, demonstrating that the DL method has clear advantages over the conventional approach in computation efficiency.

Conclusions   In this study, a DL method is employed to model ultrashort CPA in fiber. A deep convolutional neural network that consists of convolutional blocks and fully connected layers is designed to predict ultrashort pulse propagation under different initial parameters with high precision. Specifically, the paper analyzes the propagation characteristics of the chirped ultrashort pulse and the influence of initial chirp on pulse evolution. The prediction precision and computation efficiency of the proposed method are further studied under different initial pulse parameters. Without compromising

generality，the study selects the case of different initial pulse power，width，and chirp to present the testing results．The results show that the neural network constructed performs well in both prediction precision and computation efficiency．On 500 independent testing samples，the proposed deep convolutional neural network achieves normalized root-mean-square errors smaller than 0.0584 and takes less than 1/10 the computation time of the traditional split-step Fourier method．The proposed method extends the application of DL methods in laser technologies and ultrafast optics and provides an alternative for modeling ultrashort pulse propagation in fiber.

Key words nonlinear optics; optical parametric chirped pulse amplification; convolutional neural network; nonlinear Schrodinger equation